Evaluation of Marine Surface Wind Speed Observations from AMSR2 on GCOM-W Satellite

Naoto Ebuchi

***Abstract*—Observations of marine surface scalar wind speeds from the Advanced Microwave Scanning Radiometer 2 (AMSR2), onboard the Global Change Observation Mission-Water satellite (GCOM-W), were evaluated by comparisons with offshore moored buoy measurements, output from the European Centre for Medium Range Weather Forecast (ECMWF) Reanalysis Interim (ERA-Interim), and observations by the RapidScat (RSCAT) scatterometer onboard the International Space Station (ISS). In general, the AMSR2 wind speeds agreed well with the reference data. The Root Mean Square (RMS) difference between the AMSR2 and buoy measurements was 1.09 ms^{-1}, which is slightly larger than the mission goal of 1 ms^{-1}. Underestimation at low wind speeds (< 5 ms^{-1}) was found in the comparisons. The AMSR2 wind speeds were found to contain a slight scan bias; namely, wind speeds in the right swath are higher than those in the left swath by 0.2–0.3 ms^{-1}. Systematic dependence of the wind speed bias on the wind direction relative to the AMSR2 looking direction was found in a residual analysis. Results of the triple collocation analysis suggest that the random errors in the AMSR2 wind speed are less than 1 ms^{-1} and are smaller than those in the outputs from the numerical weather prediction (NWP) models, if random errors in the reference wind data (buoy, NWP, and RSCAT) are considered explicitly.**

***Index Terms*— AMSR2, GCOM-W, marine surface wind, microwave radiometer, validation**

I. Introduction

THE Global Change Observation Mission-Water (GCOM-W) satellite was launched by the Japan Aerospace Exploration Agency (JAXA) on 17 May 2012 into a sun-synchronous, 98.2° inclination, 700 km circular orbit with a local equator crossing time at the ascending node of 1:30 pm, as a member of the A-Train satellite constellation. The GCOM-W satellite carries the Advanced Microwave Scanning Radiometer 2 (AMSR2), which is a 6-band multi-frequency (6.7–89 GHz), dual-polarization (V and H) microwave radiometer and is a successor of the AMSR on the Advanced Earth Observing Satellite-II (ADEOS-II) satellite and the AMSR for NASA's Earth Observing System (AMSR-E) onboard the Aqua satellite. The AMSR2 measures microwave brightness temperature over a 1450-km-wide swath with spatial resolutions of 5–50 km depending on the frequency. The conical scan mechanism of the AMSR2 covers more than 99% of the Earth's surface every 2 days. More details of the AMSRS2 and GCOM-W were described in [1], [2].

From the multi-frequency and dual-polarized AMSR2 measurements, several parameters of the ocean, atmosphere, land, and cryosphere were retrieved through theoretical and empirical algorithms. The JAXA's standard AMSR2 data product contains the sea surface wind speed, vertically-integrated water vapor, cloud liquid water, precipitation, sea surface temperature, sea ice concentration, snow depths, and soil moisture. The AMSR2 provides global coverage of these parameters at high spatial and temporal resolution. The goal of the AMSR2 mission for the wind speed measurements is to achieve an accuracy of 1 ms^{-1} determined as a value of Root Mean Square (RMS) difference by a comparison with offshore buoy measurements [3].

Microwave radiometer measurements of surface scalar wind speeds over the global oceans have been utilized for practical applications, such as weather prediction, wave forecasting, maritime safety, and coastal management, as well as in scientific studies in the fields of meteorology, oceanography, and climate studies. Validation of the data quality and characterization of measurement errors are needed for these scientific and practical applications, since the wind speed is indirectly deduced from the microwave brightness temperatures of the sea surface. Wind data derived from spaceborne microwave sensors have been evaluated by comparisons with in situ wind measurements from buoys and vessels (e.g., [4]–[12]). Comparisons with outputs from numerical weather prediction (NWP) models have also been employed (e.g., [10], [13], [14]). Several studies made inter-comparisons of wind data from different spaceborne sensors (e.g., [10], [11], [12], [15]).

In the present study, following these approaches, the wind speeds observed by the AMSR2 onboard the GCOM-W satellite over the global oceans were evaluated by comparisons with data from offshore moored buoys, an NWP-based reanalysis dataset, and measurements by a spaceborne scatterometer. By analyzing the wind speed residuals, errors in the wind speed measurements were characterized.

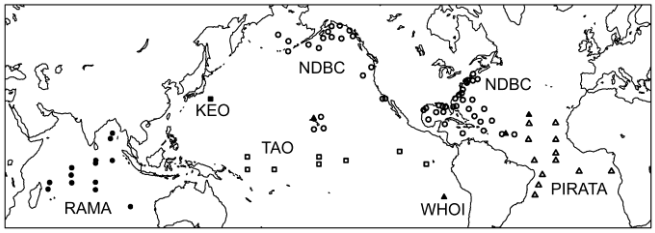

Fig. 1. Map of the offshore moored buoys used in the present study.

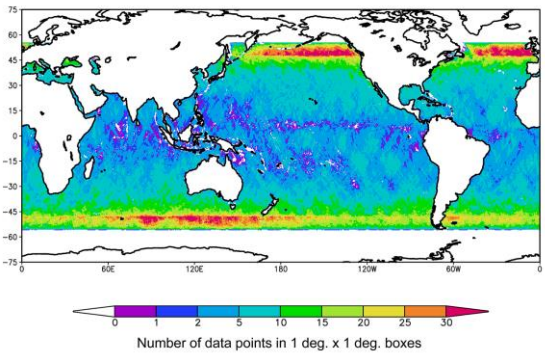

Fig. 2. Geographical distribution of the data points collocated with ISS-RSCAT observations. Number of collocated data points for a period of one month in March 2015 in boxes of 1° × 1° is shown by color.

II. Data and Methods

A. *JAXA's AMSR2 Standard Product*

The Level 2 AMSR2 Standard Products (version 2.1), downloaded from JAXA's GCOM-W Data Providing Service site (https://gcom-w1.jaxa.jp/auth.html), were utilized in this study. The spatial resolution of the wind speed data is 15 km with a spatial sampling of 10 km, and the width of the swath is 1450 km. In the JAXA's algorithm, the wind speeds are retrieved mainly from the brightness temperature measurements at 36.5 and 6.9 GHz by the AMSR2 [16]. The derived wind speeds are considered to correspond to the equivalent-neutral wind speeds at a height of 10 m above the sea surface. More details of the wind products are described in the Algorithm Theoretical Basis Document (ATBD) [16]. Data obtained over a period of two years from August 2013 to August 2015 were utilized in this study. All of the flagged data, including the rain flag, were discarded. Only the data obtained under the condition of rain rate less than 0.5 mm h^{-1} were used in the analysis.

B. *Offshore Moored Buoys*

Wind data obtained from offshore moored buoys operated by the National Data Buoy Center, National Oceanic and Atmospheric Administration (NOAA/NDBC), Tropical Atmosphere and Ocean (TAO) Project, Prediction and Research Moored Array in the Atlantic (PIRATA) Project, Research Moored Array for African-Asian-Australian Monsoon Analysis and Prediction (RAMA) Project, the Woods Hole Oceanographic Institution (WHOI), and the Kuroshio Extension Observatory (KEO) Project were downloaded from the websites of these data providers and compared with the AMSR2 observations. The locations of the buoys are shown in Fig. 1. Only the buoys moored in deep water (> 50 m) far from the coast (> 50 km) were selected. Most of the buoys measured the 10-minute average wind speed continuously. Buoys operated by the Japan Agency for Marine-Earth Science and Technology (JAMSTEC), such as the Triangle Trans-Ocean buoy Network (TRIRON) buoys, were not used in this study, because the sampling and averaging schemes were different from those of the other buoys.

The wind speeds observed by the buoys were converted to the 10-m height equivalent-neutral wind speed by height and stability corrections using the code provided by [17]. The AMSR2 wind data were collocated with the buoy data in time and space allowing temporal and spatial separations of 5 minutes and 7.5 km, respectively, since these values were half of the sampling interval of the buoy measurements and spatial resolution of AMSR2 observations. Only the AMSR2 wind data closest to the buoy location in space and the buoy data closest to the AMSR2 observation in time were used.

C. *ERA-Interim*

Wind data from the European Centre for Medium Range Weather Forecast (ECMWF) Reanalysis Interim (ERA-Interim) were collocated in space and time with the AMSR2 observations. The spatial and temporal resolution of the ERA-Interim data are 0.75° and 6 hours, respectively. According to [18], data from AMSR2 were not used in the ERA-Interim. Data from a period of three months from January to March 2015 were used in this study. The zonal and meridional wind components from the ERA-Interim were linearly interpolated in space and time to the AMSR2 observations. Only the data observed between 60 °S and 60 °N were used in order to avoid contamination by undetected sea ice. The number of collocated data points was approximately 302 million. It should be noted that the ERA-Interim winds are "real" winds rather than equivalent-neutral winds. In general, the difference between the 10-m equivalent-neutral and real (non-equivalent-neutral) wind speeds is estimated to be 0.2 ms^{-1} as the global average [19], [20].

D. *RapidScat on ISS*

The RapidScat (RSCAT) is a Ku-band microwave scatterometer onboard the International Space Station (ISS) and is a replacement of QuikScat. It provides marine surface vector wind fields with a spatial sampling of 12.5 km across a swath of 900 km. The orbit of the ISS is non-sun-synchronous with an inclination angle of 51.6° and an altitude of 435 km. The RSCAT wind data (RapidScat Level 2B Ocean Wind Vectors in 12.5 km Slice Composites, version 1.2) over a period of three months from January to March 2015 were obtained from the National Aeronautics and Space Administration (NASA) Jet Propulsion Laboratory (JPL) Physical Oceanography Distributed Active Archive Center (PO.DAAC). The accuracy

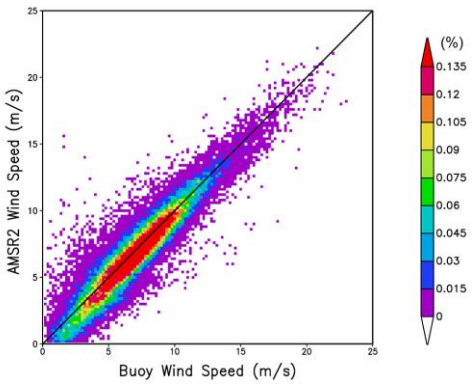

Fig. 3. Comparison of AMSR2 wind speeds with buoy measurements. Number density relative to the total number (%) in boxes of 0.2 × 0.2 ms^{-1} is shown by color.

of wind speeds measured by the RSCAT was reported as 1.1 ms^{-1} by comparisons with buoy observations [21]. Wind data from the National Centers for Environmental Prediction (NCEP) Numerical Weather Prediction (NWP) model collocated in space and time with the RSCAT observations are also contained in the RSCAT wind products. The NCEP wind is considered as the 10-m real (non-equivalent-neutral) wind.

The RSCAT and AMSR2 wind observations were collocated to temporal and spatial separations of 60 minutes and 12.5 km, respectively. Only the RSCAT wind vector cell closest to the AMSR2 observation in time and space was kept in the collocated data set. All of the flagged data, including the rain flag, were discarded. The data flagged by any of the AMSR2 and RSCAT rain flags were omitted from the collocated data set to remove data contaminated by rain.

Figure 2 shows the distribution of the collocated data for a period of one month in March 2015. Regions of higher data density are located around latitudes of 50°, because of the low inclination of the ISS orbit. In the tropical convergence zones, the number of collocated data points is fewer, because the AMSR2 and RSCAT data containing rain flags were discarded. When discussing and interpreting results from comparisons with the RSCAT data, we should consider the uneven

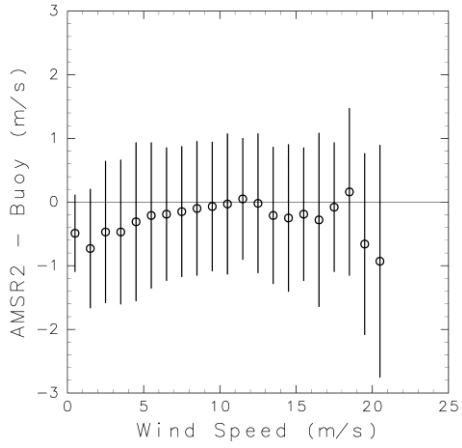

Fig. 4. Dependence of the wind speed residuals (AMSR2 − buoy) on the average wind speed of AMSR2 and buoy. Averages and standard deviations are shown in bins of 1 ms^{-1}.

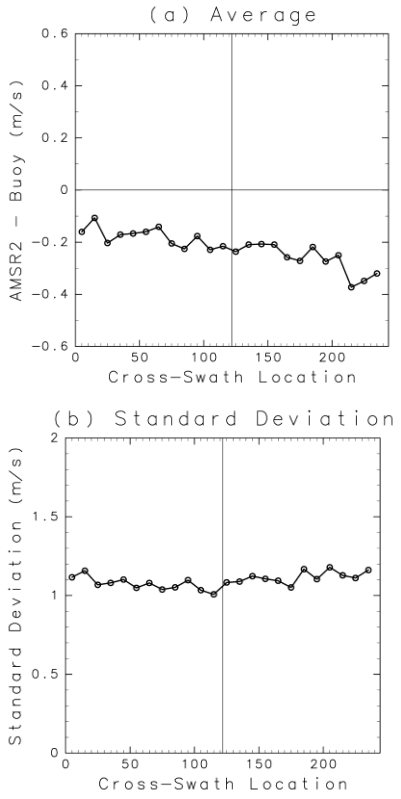

Fig. 5. Dependence of the wind speed residuals (AMSR2 − buoy) on the cross-swath location. (a) Average and (b) standard deviation of the wind speed residuals. Scan number 1 in the x-axis corresponds to the outer edge of the right swath, while 242 corresponds to the outer edge of the left swath. The vertical bar indicates the nadir.

geographical distribution of the spatial locations from which the data was obtained as shown in Fig. 2.

III. Results and Discussion

A. Comparison with Buoy Data

Figure 3 shows the comparison of the AMSR2 and buoy wind speed measurements. The total number of collocated data points is 54,196. Figure 3 shows the number density of data points (% of the total number) in 0.2 × 0.2 ms^{-1} boxes. The AMSR2 wind speed is in close agreement with the 10-m height equivalent-neutral wind speed derived from the buoy observations. The bias (AMSR2 − buoy) and RMS difference were −0.22 and 1.09 ms^{-1}, respectively. The RMS difference is very close to, but slightly exceeds, the mission goal of 1 ms^{-1}. In Fig. 3, there is a discernible underestimation of low wind speeds (< 5 ms^{-1}).

In Fig. 4, the residual wind speed (AMSR2 − buoy) is plotted against the wind speed, which is taken as an average of the buoy and the AMSR2 wind speeds to avoid a spurious bias due to the asymmetry of the distribution of the data points at very low wind speeds [22]. The mean and standard deviation of the residual wind speeds in bins of 1 ms^{-1} were calculated (Fig. 4). As in Fig. 3, a negative bias can be seen of up to 0.7 ms^{-1} for wind speeds less than 5 ms^{-1}. The large negative bias for wind speeds over 20 ms^{-1} is possibly due to uncertainties in the

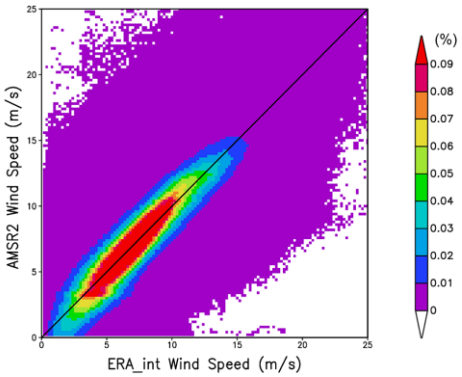

Fig. 6. Comparison of AMSR2 wind speeds with the ERA-Interim reanalysis. Number density relative to the total number (%) in boxes of 0.2 × 0.2 ms^{-1} is shown by color.

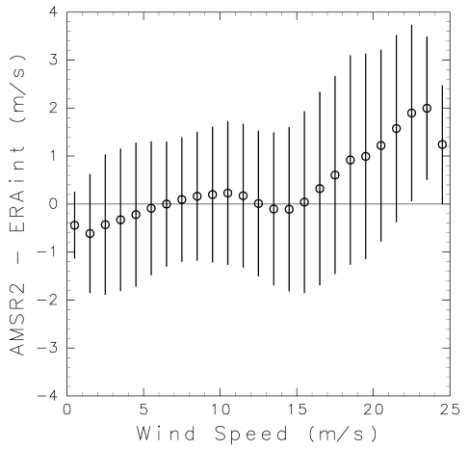

Fig. 7. Dependence of the wind speed residuals (AMSR2 - ERA Interim) on the average wind speed of the AMSR2 and ERA-Interim. Averages and standard deviations are shown in bins of 1 ms^{-1}.

geophysical model used in the AMSR2 wind retrieval under extreme wind conditions together with the sparsity of the collocated data and the unreliability of measurements from buoys at high wind speeds [23].

The averages and standard deviations of the wind speed residuals are plotted as a function of cross-swath location in Fig. 5 to assess possible scan bias in the AMSR2 wind speeds. The AMSR2 conically scans the Earth's surface counter-clockwise, and measures the brightness temperatures in the forward direction only. Scan number 1 in the x-axis of Fig. 5 corresponds to the outer edge of the right swath (75° right to the flight direction), and scan number 242 corresponds to the outer edge of the left swath (75° left to the flight direction). The bias (AMSR2 − buoy) decreases from right to left across the swathes with an amplitude of 0.3 ms^{-1}, suggesting errors in the calibration of the brightness temperature measurements by AMSR2, while the standard deviation does not vary with the cross-swath location. It can be conjectured that errors in the attitude of the spacecraft and/or alignment of the sensor may cause errors in the incidence angle resulting in the scan bias.

By using the dataset collocated with buoy observations, correlations of the wind speed residual with other physical quantities at the air-sea interface, such as air and sea surface temperatures, air-sea temperature difference, humidity, significant wave height, and wave age, were calculated (the results are not shown). However, no significant correlations were found. In addition, no significant correlations between the wind speed residuals and other variables derived from the AMSR2 brightness temperature, such as the sea surface temperature, integrated water vapor content, and cloud liquid water content, were discernible. These results indicate that the AMSR2 wind retrieval algorithm successfully separated the dependence of brightness temperature on wind speed from the dependencies on other atmosphere and oceanic variables.

B. Comparison with ERA-Interim Data

Figure 6 shows the comparison of the AMSR2 wind speeds with the ERA-Interim data. The total number of collocated data points is 302,216,252. The figure shows the number density (% of the total number) in 0.2 × 0.2 ms^{-1} boxes. It is confirmed that the AMSR2 wind speed agrees well with the ERA-Interim reanalysis data. The bias (AMSR2 − ERA-Interim) and RMS difference were −0.03 and 1.48 ms^{-1}, respectively. The difference in the biases between the comparisons with the buoy and ERA-Interim data corresponds to the global difference of equivalent-neutral (buoy) and real (ERA-Interim) wind speeds. The value of the RMS difference is larger than that for the buoy comparison. The coarse temporal and spatial resolutions of the ERA-Interim dataset and interpolation in time and space might increase the RMS difference. A similar trend of underestimation at low wind speeds (< 5 ms^{-1}) is also discernible, as seen in the comparison with buoy data (Fig. 3).

In Fig. 7, the residual wind speed (AMSR2 – ERA-Interim) is plotted against the wind speed, which is taken as an average of the ERA-Interim and AMSR2 wind speeds to avoid a spurious bias, as in Fig. 4. The mean and standard deviation of the residual wind speeds in bins of 1 ms^{-1} were calculated. As seen in the comparison with buoy data (Fig. 4), a negative bias is found for wind speeds lower than 5 ms^{-1}, although the amplitude is slightly smaller. The bias at very high wind speed showed a different trend from that in the comparison with buoy data. The reliability of the ERA-Interim data at very high wind speeds is also questionable, because parameterization of the surface boundary layer under high wind wave conditions is questionable, and the coarse spatial resolution and temporal and spatial interpolations may smear the high wind.

As in Fig. 5, averages and standard deviations of the wind speed residuals are plotted as a function of the cross-swath location in Fig. 8 to assess the scan bias. It is confirmed that the residual (AMSR2 – ERA-Interim) decreases from right to left across the swath with an amplitude of a few tenths of ms^{-1}, while the standard deviation does not vary with the cross-swath location. The residuals in the ascending paths in the Southern Hemisphere showed a different feature in the left swath (scan numbers 122–242), since observations contaminated by the sun glitter were discarded.

The difference of bias between the Northern and Southern Hemisphere is also discernible in Fig. 8. Although it is difficult

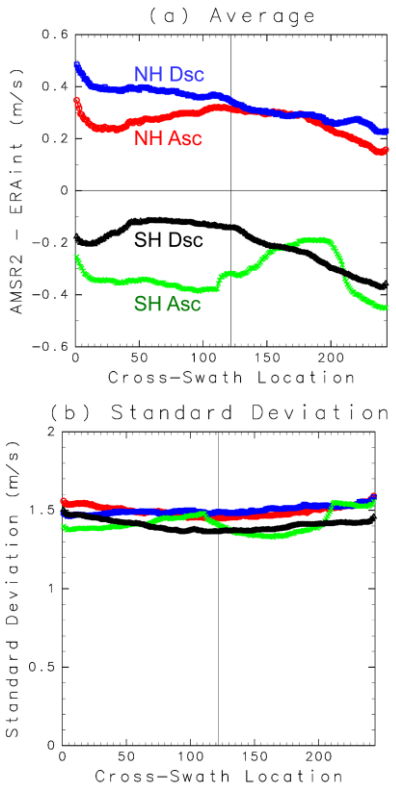

Fig. 8. Dependence of the wind speed residuals (AMSR2 − ERA Interim) on the cross-swath location. (a) Average and (b) standard deviation of the wind speed residuals. Scan number 1 in the x-axis corresponds to the outer edge of the right swath, while 242 corresponds to the outer edge of the left swath. The vertical bar indicates the forward look. "NH" and "SH" denote the Northern and Southern Hemispheres, respectively, and "Asc" and "Dsc" denote the ascending and descending paths, respectively.

to specify the reason, it can be conjectured that differences in sampling and wind speed dependent bias in the AMSR2 winds relative to the ERA-Interim winds might cause the difference. In the analysis, data obtained in the period from January to March, which corresponds to the boreal summer and austral winter, were used. Data obtained in the Northern Hemisphere contained relatively higher wind speeds (see also Fig. 10) resulting in positive bias relative to the ERA-Interim winds (Fig. 7). This might cause the positive bias in the Northern Hemisphere shown Fig. 8.

As mentioned above, a large portion of data obtained in the ascending orbits at low to mid latitudes in the Southern Hemisphere, where relatively lower winds were observed, were contaminated by sun glint and removed from the analysis. This might cause a hump in the left swath (scan number 120-200) in Fig. 8.

Figure 9 shows the wind speed residuals as a function of the ERA-Interim wind speed and relative azimuth angle between the ERA-Interim wind direction and AMSR2-looking direction. The residuals were averaged in bins of 1 ms^{-1} in wind speed and 5° in the relative wind direction. The wind speed residuals clearly exhibited a symmetrical dependence on the relative wind direction. The amplitude is approximately 0.6 m^{-1} at wind speeds of 10 ms^{-1}. As pointed out by [24], the brightness temperatures of the sea surface depends on the wind direction

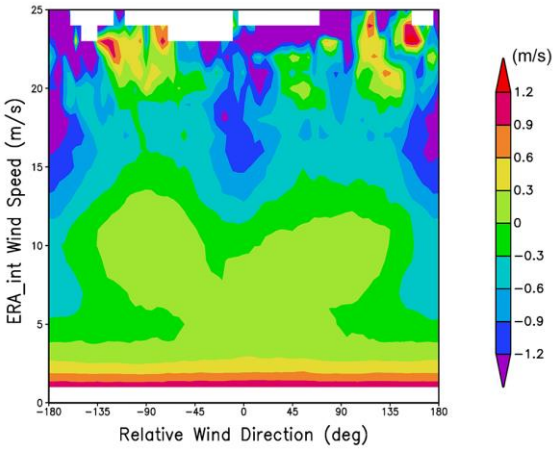

Fig. 9. Dependence of the wind speed residuals (AMSR2 – ERA-Interim) on the ERA Interim wind speed and wind direction relative to the AMSR2-looking direction.

relative to the sensor-looking direction. In the JAXA's algorithm, this effect is compensated by the difference of brightness temperatures between the V and H polarizations [16]. The result in Fig. 9 implies that the wind speed retrieval algorithm needs further improvements to reduce the influence of the dependence of the brightness temperatures on the relative wind direction.

From the AMSR2-ERA-Interim collocated dataset, global wind speed histograms were calculated in bins of 1 ms^{-1} (Fig. 10). The two histograms from the AMSR2 and ERA-Interim wind data generally agree with each other in the ascending/descending paths and the Northern/Southern Hemispheres. However, slight discrepancies are found at low wind speeds. The AMSR2 wind showed an excess of low wind speed data compared with the ERA-Interim data, indicating underestimation of low wind speeds, as seen in the comparisons with the buoy and ERA-Interim wind data.

C. Comparison with RSCAT Data

In Fig. 11, the comparison of the AMSR2 and RSCAT wind speeds are plotted as the number density (% to the total number of data points, 3,850,522) in boxes of 0.2 × 0.2 ms^{-1}. Note that the geographical distribution of data points is not uniform (Fig. 2). It is confirmed that the AMSR2 wind speeds generally agree with the measurements from the RSCAT, although systematic underestimation is again discernible at low wind speeds, as in Figs. 3 and 6. The bias (AMSR2 − RSCAT) and RMS difference were −0.34 and 1.20 ms^{-1}, respectively. The temporal separation of 60 minutes might have increased the RMS difference, compared to that with the buoy data in Fig. 3.

Figure 12 shows the dependence of wind speed residual (AMSR2 − RSCAT), as in Fig. 4 and 7. The result confirmed the negative bias in the low wind speed range. At very high wind (> 15 ms^{-1}), the AMSR2 wind speed is significantly lower than the RSCAT wind, in contrast with the results in Figs. 4 and 7. In the very high wind range, model functions to retrieve wind speed from backscattered cross sections (scatterometers) and

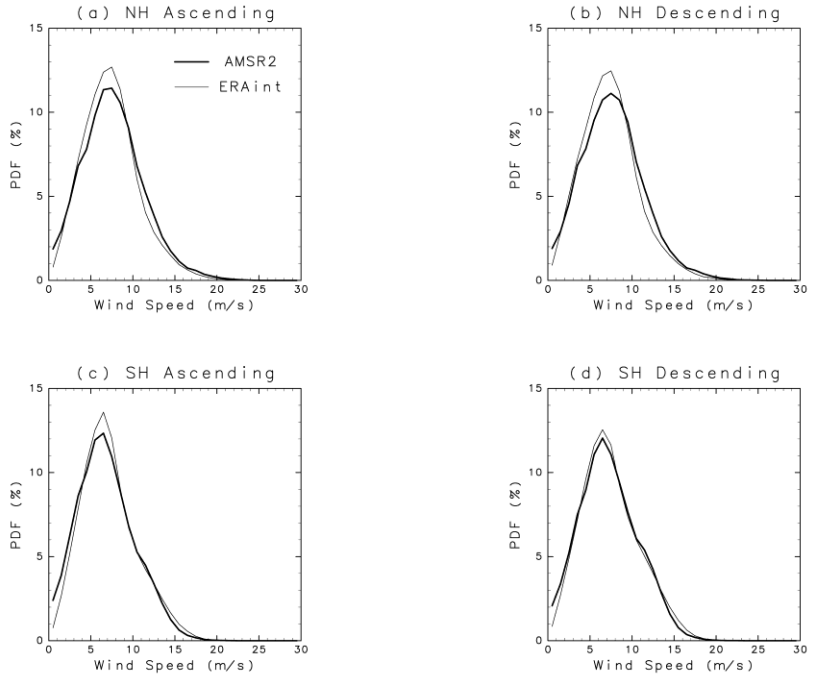

Fig. 10. Comparisons of global wind speed histograms. Number density relative to the total number of data points (in %) is shown in bins of 1 ms-1. (a) Ascending paths in the Northern Hemisphere, (b) descending paths in the Northern Hemisphere, (c) ascending paths in the Southern Hemisphere, and (d) descending paths in the Southern Hemisphere.

brightness temperatures (microwave radiometers) may not be calibrated accurately, since we cannot obtain reliable reference wind data (e.g., [22]). Buoy measurements are easily suffered from tilting effects and flow separation by high waves. Wind measured by vessels and offshore platforms may be affected by flow distortion by the large structure. Outputs from NWP models may have limitations in spatial and temporal resolutions to smear the high winds. Further investigations using other techniques to measure the high winds, such as dropsondes and airborne stepped frequency microwave radiometer, are needed to evaluate the performance of AMSR2 under the very high wind conditions.

In residual analyses of the dataset collocated with RSCAT winds, very similar results concerning the trends in the scan bias were found as in Figs. 5 and 8, although the results are not shown here. Dependence of wind speed bias on the relative wind direction similar to Fig. 9 was also confirmed by the data sets collocated with RSCAT (not shown).

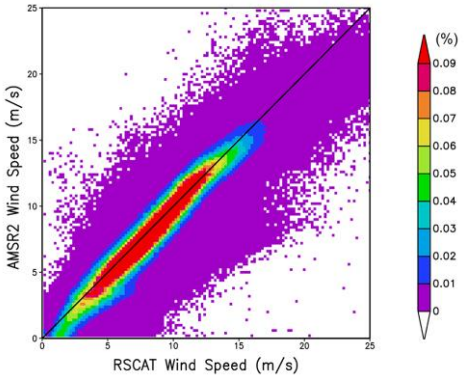

Fig. 11. Comparison of AMSR2 wind speeds with RSCAT data. Number density relative to the total number (%) in boxes of 0.2 × 0.2 ms^{-1} is shown by color.

D. Triple Collocation Analysis

In most validation studies, including the previous subsections, errors in the reference wind data, such as buoy measurements and NWP outputs, are assumed to be negligibly small. However, this assumption is not always valid. Triple collocation analysis [25], [26] has been utilized to explicitly evaluate the errors in the reference data. By using the collocated datasets analyzed in the previous sections, triple collocation was applied to quantify the random errors in the AMSR2 and

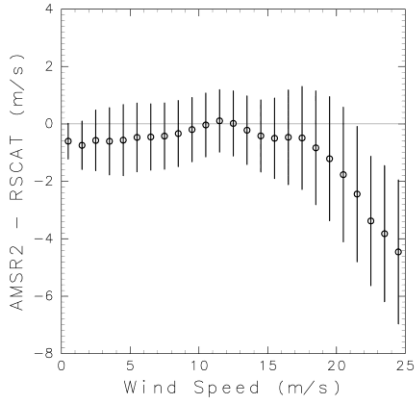

Fig. 12. Dependence of the wind speed residuals (AMSR2 - RSCAT) on the average wind speed of the AMSR2 and RSCAT. Averages and standard deviations are shown in bins of 1 ms^{-1}.

other wind measurements.

Following [25],

$$\begin{aligned} x &= t + \delta_x, \\ y &= s_y(t + \delta_y), \\ z &= s_z(t + \delta_z), \end{aligned} \tag{1}$$

where x, y, and z are three collocated measurements of the same variable by different methods; t is the unknown "true" value for x, y, and z; δ_x, δ_y, and δ_z are random errors in the measurements of x, y, and z; and s_y and s_z are the scaling (calibration) constants of y and z relative to x. Relative biases among x, y, and z have been removed by subtracting their averages.

It is assumed that

$$\langle \delta_x \rangle = \langle \delta_y \rangle = \langle \delta_z \rangle = 0, \tag{2}$$

and

$$\begin{aligned} \langle \delta_x{}^2 \rangle &= \varepsilon_x{}^2, \\ \langle \delta_y{}^2 \rangle &= \varepsilon_y{}^2, \\ \langle \delta_z{}^2 \rangle &= \varepsilon_z{}^2, \end{aligned} \tag{3}$$

where < > denotes the average, and ε_x, ε_y, and ε_z are the standard deviations of the errors in the measurements of x, y, and z, respectively. Assuming that the random errors in x, y, and z are independent with each other and the true value t, i.e.,

$$\begin{aligned} &\langle \delta_x \, \delta_y \rangle = \langle \delta_y \, \delta_z \rangle = \langle \delta_z \, \delta_x \rangle = 0, \\ &\langle t \, \delta_x \rangle = \langle t \, \delta_y \rangle = \langle t \, \delta_z \rangle = 0, \end{aligned} \tag{4}$$

the values of ε_x, ε_y, ε_z, s_y, and s_z were estimated by calculating the variance and covariance of x, y, and z.

Table I shows the results of the triple collocation for various combinations of the wind data with the AMSR2 observations. The errors in the buoy and RSCAT wind data showed the lowest values, while the ERA-Interim and NCEP datasets exhibited larger errors. The standard deviation of errors in the AMSR2 wind speeds is slightly less than 1 ms^{-1}, which is larger than those in the buoy and RSCAT data but smaller than those in the NWP outputs (ERA-Interim and NCEP), although the values of the standard deviations vary with the choice of dataset. The results imply that the standard deviations were smaller than the RMS differences obtained in the previous subsections, if errors in the reference wind data (buoy, RSCAT, and NWP) are considered explicitly. However, it should be noted that the buoy data have likely been assimilated into the NWP models and the assumption of uncorrelated errors in Eq. (4) may not be fully satisfied.

TABLE I
SCALING CONSTANTS AND STANDARD DEVIATION OF RANDOM ERRORS ESTIMATED BY TRIPLE COLLOCATION.

(a) Number of data points = 1,761

	Data	Scaling Constants	Standard Deviation (ms^{-1})
x	Buoy	1.000	0.782
y	ERA-Interim	1.046	1.100
z	AMSR2	0.898	0.931

(b) Number of data points = 1,574,077

	Data	Scaling Constants	Standard Deviation (ms^{-1})
x	RSCAT	1.000	0.772
y	ERA-Interim	1.007	1.304
z	AMSR2	0.972	0.889

(c) Number of data points = 1,578,366

	Data	Scaling Constants	Standard Deviation (ms^{-1})
x	RSCAT	1.000	0.730
y	NCEP	1.003	1.695
z	AMSR2	1.104	0.926

IV. SUMMARY AND CONCLUDING REMARKS

In this study, the JAXA's Level-2 AMSR2 wind speed measurements (version 2.1) were evaluated by comparisons with data from offshore moored buoys, the ERA-Interim reanalysis dataset, and observations from the ISS-RapidScat scatterometer. In general, the AMSR2 wind showed good agreement with the data. However, the RMS difference with buoy measurements was 1.09 ms^{-1}, which is slightly larger than the mission goal of 1 ms^{-1}. Systematic underestimation of low wind speeds (< 5 ms^{-1}) was also identified.

At high wind range (> 15 ms^{-1}), the comparisons with buoy, ERA-Interim and RSCAT data showed controversial results. AMSR2 wind speeds are much higher than the ERA-Interim winds and much lower than RSCAT winds. At this wind range, we may not obtain reliable reference wind data due to various problems in the measurement techniques and NWP modellings. Further studies using other measurement techniques, such as dropsondes and airborne stepped frequency microwave radiometer, are needed to evaluate the performance of spaceborne microwave radiometers and scatterometers in the high wind range.

A small scan bias was detected in the AMSR2 winds, namely, wind speeds at the right of the swath are higher than those at the left of the swath by a few tenths of ms^{-1}. It was also shown that the wind speed residuals depend on the wind direction relative to the sensor-looking direction. Results of the triple collocation suggested that the accuracy of the AMSR2 wind is better than 1 ms^{-1}, if random errors in the reference wind data (buoy and NWP) were considered explicitly.

In conclusion, the accuracy of the JAXA's AMSR2 version 2.1 wind data is very close to the mission goal, but still needs further improvements. Reflecting on the results from validation studies, refinements to the AMSR2 wind retrieval algorithm and the development of version 3 are now underway. The new dataset will be distributed in March 2017. Accurate wind speed data with high spatial and temporal resolution are highly useful to a wide range of scientific studies and operational

applications in various fields.

ACKNOWLEDGMENT

The author wishes to express his gratitude to Haruhisa Shimoda (Tokai University), Taikan Oki (The University of Tokyo/JAXA), Akira Shibata (The Remote Sensing Technology Center of Japan, RESTEC), Keiji Imaoka (Yamaguchi University), Misako Kachi, and Takashi Maeda (JAXA) for providing data and information of AMSR2 and GCOM-W. The present study is supported by the JAXA under the GCOM project. Discussions with colleagues at the GCOM PI workshops were very helpful. The wind data products used in this paper were downloaded from the ftp sites of JAXA, ECMWF, and NASA PO.DAAC at JPL. Figures in this paper were produced by the Grid Analysis and Display System (GrADS) and the GFD-DENNOU Library.

REFERENCES

[1] K. Imaoka, M. Kachi, H. Fujii, H. Murakami, M. Hori, A. Ono, T. Igarashi, K. Nakagawa, T. Oki, Y. Honda, H. Shimoda, "Global Change Observation Mission (GCOM) for Monitoring Carbon, Water Cycles, and Climate Change," *Proc. IEEE*, vol. 98, no. 5, pp. 717 - 734, doi: 10.1109/JPROC.2009.2036869, 2010.

[2] H. Shimoda, "GCOM science overview," *Proc. IGARSS 2015*, Milan, Italy, July 2015, pp. 5091 - 5094, doi: 10.1109/IGARSS.2015.7326978, 2015.

[3] JAXA, "GCOM mission requirement specifications," *JAXA Tech. Doc.*, SAP-060001, 2006 (in Japanese).

[4] F. J. Wentz, "Measurement of oceanic wind vector using satellite microwave radiometers," *IEEE Trans. Geosci. Remote Sens.*, vol. 30, no. 5, pp. 960 - 972, doi: 10.1109/36.175331, 1992.

[5] M. A. Bourassa, D. M. Legler, W. T. Liu, and J. J. O'Brien, "Wind observations from new satellite and research vessels agree," *EOS Trans. AGU*, vol. 78, no. 51, pp. 597-597, 1997.

[6] C. Rufenach, "Comparison of four ERS-1 scatterometer wind retrieval algorithms with buoy measurements," *J. Atmos. Oceanic Tech.*, vol. 15, no. 1, pp. 304-313, 1998.

[7] M. H. Freilich, and R. S. Dunbar, "The accuracy of the NSCAT-1 vector winds: Comparison with NDBC buoys," *J. Geophys. Res.*, vol. 104, no. C5, pp. 11,231-11,246, 1999.

[8] F. J. Wentz, and T. Meissner, "AMSR Ocean Algorithm, Version 2," *RSS Report*, no. 121599A-1, 66 pp., Remote Sensing Systems, Santa Rosa, CA, USA, 66 pp., 2000.

[9] N. Ebuchi, H. C. Graber, and M. J. Caruso, "Evaluation of wind vectors observed by QuikSCAT/SeaWinds using ocean buoy data," *J. Atmos. Oceanic Tech.*, vol. 19, no. 12, pp. 2049-2062, 2002.

[10] F. J. Wentz, T. Meissner and D. Smith, "Evaluation of microwave scatterometers and radiometers as satellite anemometers," *Proc. IGARSS 2005*, Anchorage, Alaska, U.S.A, September 2004, pp. 3310-3313, doi: 10.1109/IGARSS.2005.1526549, 2004.

[11] A. Bentamy, D. Croize-Fillon, and C. Perigaud, "Characterization of ASCAT measurements based on buoy and QuikSCAT wind vector observations," *Ocean Sci.*, vol. 4, no. 4, pp. 265-274, 2008.

[12] N. Ebuchi, "Evaluation of wind speed observed by AMSR using data from ocean buoys and SeaWinds," *J. Remote Sens. Soc. Jpn*, vol. 29, no. 1, pp. 174-178, 2009.

[13] A. Stoffelen, "A simple method for calibration of a scatterometer over the ocean," *J. Atmos. Oceanic Technol.*, vol. 16, pp. 275-282, 1999.

[14] J. Verspeek, A. Stoffelen, M. Portabella, H. Bonekamp, C. Anderson, and J. Figa Saldaña, "Validation and calibration of ASCAT using CMOD5.n," *IEEE Trans. Geosci. Remote Sens.*, vol. 48, no. 1, pp. 386-395, 2010.

[15] N. Ebuchi, "Evaluation of wind speed globally observed by AMSR2 on GCOM-W1," *Proc. IGARSS 2014*, Quebec City, Quebec, Canada, July 2014, pp. 3902-3905, doi: 10.1109/IGARSS.2014.6947337, 2014.

[16] Earth Observation Research Center, Japan Aerospace Exploration Agency, "Descriptions of GCOM-W1 AMSR2, Level 1R and Level 2 Algorithms," NDX-120015A, Japan Aerospace Exploration Agency, Tsukuba, Japan, 119 pp., 2013.

[17] W. T. Liu, and W. Q. Tang, "Equivalent neutral wind," *JPL Publ.* 96-19, Jet Propul. Lab., Pasadena, CA, USA, 8 pp., 1996.

[18] D. P. Dee, S. M. Uppala, A. J. Simmons, P. Berrisford, P. Poli, S. Kobayashi, U. Andrae, M. A. Balmaseda, G. Balsamo, P. Bauer, P. Bechtold, A. C. M. Beljaars, L. van de Berg, J. Bidlot, N. Bormann, C. Delsol, R. Dragani, M. Fuentes, A. J. Geer, L. Haimberger, S. B. Healy, H. Hersbach, E. V. Hólm, L. Isaksen, P. Kållberg, M. Köhler, M. Matricardi, A. P. McNally, B. M. Monge-Sanz, J.-J. Morcrette, B.-K. Park, C. Peubey, P. de Rosnay, C. Tavolato, J.-N. Thépaut and F. Vitart, "The ERA-Interim reanalysis: configuration and performance of the data assimilation system," *Q. J. R. Meteorol. Soc.*, vol. 137, pp. 553–597, 2011.

[19] A. Verhoef, M. Portabella, A. Stoffelen, and H. Hersbach, "CMOD5.n—The CMOD5 GMF for Neutral Winds," *EUMETSAT Tech. Note*, SAF/OSI/CDOP/KNMI/TEC/TN/165, 13 pp., 2008.

[20] H. Hersbach, "CMOD5.N: A C-band geophysical model function for equivalent neutral wind," *Technical Memorandum*, ECMWF, no. 554, 20 pp., 2008.

[21] N. Ebuchi, "Evaluation of marine vector winds observed by RapidScat on the International Space Station using statistical distribution," *Proc. IGARSS 2015*, Milan, Italy, July 2015, pp. 4901-4904, doi: 10.1109/IGARSS.2015.7326930, 2015.

[22] M. H. Freilich, "Validation of vector magnitude datasets: Effects of random component errors," *J. Atmos. Oceanic Tech.*, vol. 17, pp. 695-703, 1997.

[23] W. J. Pierson, "Examples of, reasons for, and consequences of the poor quality of wind data from ships for the marine boundary layer: Implications for remote sensing," *J. Geophys. Res.*, vol. 95, no. C8, pp. 13313–13340, 1990.

[24] F. J. Wentz, "Measurement of oceanic wind vector using satellite microwave radiometers," *IEEE Trans. Geosci. Remote Sens.*, vol. 30, no 5, pp. 960-972, 1992.

[25] A. Stoffelen, "Toward the true near-surface wind speed: Error modeling and calibration using triple collocation," *J. Geophys. Res.*, vol. 103, no. C4, pp. 7755-7766, 1998.

[26] W. Lin, M. Portabella, A. Stoffelen, J. Vogelzang, and A. Verhoef, "ASCAT wind quality under high subcell wind variability conditions," *J. Goephys. Res.*, vol. 120, no. C8, pp. 5804-5819, doi: 10.1002/2015JC010861, 2015.

Naoto Ebuchi received the B.S., M.S., and D.Sc. degrees in geophysics in 1984, 1986, and 1992 from Tohoku University, Sendai, Japan. He is currently a professor and the Director of the Institute of Low Temperature Science, Hokkaido University, Sapporo, Japan. His research interests include physical processes of microwave backscattering and radiation from the sea surface and applications of active and passive microwave sensors, such as microwave scatterometers, microwave radiometers, radar altimeters, and synthetic aperture radars, to observations of the air-sea boundary processes.